Available online at www.sciencedirect.com
SCIENCE DIRECT®
Journal of Sound and Vibration 285 (2005) 1039–1048
JOURNAL OF SOUND AND VIBRATION
www.elsevier.com/locate/jsvi

Contactless liquid detection in a partly filled tube by resonance

M.A. Jacobs[a], R. Breeuwer[b], M.F. Kemmere[a,*], J.T.F. Keurentjes[a]

[a]*Process Development Group, Department of Chemical Engineering and Chemistry, Eindhoven University of Technology, P.O. Box 513, Den Dolech 2, 5600 MB Eindhoven, Netherlands*
[b]*Department of Imaging and Data Interpretation, TNO TPD, Netherlands Organization for Applied Scientific Research, P.O. Box 155, 2600 AD Delft, Netherlands*

Received 8 March 2004; received in revised form 31 August 2004; accepted 14 September 2004
Available online 2 December 2004

Abstract

Contactless fluid level detection in process equipment is an important challenge for the process automation industry, especially under high-pressure conditions. In this study, a method is presented, which permits the contactless measurement of liquid levels in thin opaque capillaries at high pressures. The method is based on the mass dependence of the flexural resonance frequencies of a finite section of a tube. These resonance frequencies are determined from the complex electrical impedance of a slitted toroid coil exciting a magnet attached to the tube. The system has been theoretically described using a set of two Bernoulli–Euler beams, resulting in an analytical solution for the equation of motion. To validate the model, experiments have been performed on a thick-walled stainless steel capillary partly filled with mercury. The model is in good agreement with the experimental data. Moreover, the sensitivity of the method appears to be adequate as a fluid level indicator for control purposes in industrial applications.

1. Introduction

In a growing number of chemical and pharmaceutical processes, near critical and supercritical fluids are replacing traditional organic solvents. In particular, high-density carbon dioxide is

*Corresponding author. Tel.: +31 40 2473673; fax: +31 40 2446104.
E-mail address: m.f.kemmere@tue.nl (M.F. Kemmere).

0022-460X/$ - see front matter © 2004 Elsevier Ltd. All rights reserved.
doi:10.1016/j.jsv.2004.09.009

increasingly used in applications such as extractions [1], polymer synthesis and processing [2] as well as pharmaceutical processing [3,4]. Depending on the fluid used, these processes are operated at much higher pressures than conventional processes, typically above 5.0 MPa. Additionally, in pharmaceutical and food processes, contactless setups are preferred, to reduce the risk of contamination. Consequently, constraints are imposed on the process equipment, including the methods for liquid level detection.

For the detection of liquids in opaque tubes at fixed positions, a technique based on the intensity of a focused ultrasonic sound beam transmitted through the tube can be used [5]. However, the resolution of signal sharply decreases with increasing wall thickness of the tubing, rendering the technique unsuitable for high-pressure systems. In this contribution, a technique is presented for the detection of variable liquid levels under high pressures. The method is based on a new implementation of the well-known effect of lowering the resonance frequency of an elastic body by mass loading. For this purpose, a section of the tube is clamped at two points and a tiny magnet is attached to the center. A slitted toroid coil excites the section of the tube in transversal resonance. The complex electrical impedance of this same coil is used to determine the resonance frequency. This enables a constructionally simple and contactless setup. Moreover, the method allows for measurements in thin, opaque capillaries, at high pressures and increased temperatures.

To determine the sensitivity of the system, it has been described as a set of two Bernoulli–Euler beams, under the assumption of free vibration. An analytical solution for the equation of motion has been derived. To validate the model, experiments with a realistic stainless steel capillary partly filled with mercury are presented.

2. Theory

In Fig. 1 a clamped tube partly filled with liquid is shown, which is considered to be in free vibration. The length between the clamps is defined L. The liquid–gas interface in the tube is marked by an abrupt change in mass density from m_1 to m_2 and is positioned at the origin. The distance between the origin and the bottom clamp is defined l_d. The system can be regarded as a set of two Bernoulli–Euler beams, each with a uniform bending stiffness EI and a constant mass density m_i [6,7]. The equation of motion is given by

$$EI\frac{\partial^4 y_i}{\partial x^4} + m_i\frac{\partial^2 y_i}{\partial x^2} = 0, \tag{1}$$

with m_i

$$m_i = \begin{cases} m_1, & -l_d < x < 0, \\ m_2, & 0 < x < L - l_d. \end{cases} \tag{2}$$

The solutions of Eq. (1) are $y_1(x, t)$ in the range $-l_d < x < 0$ and $y_2(x, t)$ in the range $0 < x < L - l_d$. The boundary conditions at $x = -l_d$ and $x = L - l_d$ are given by

$$y_1(-l_d, t) = y_1'(-l_d, t) = y_2(L - l_d, t) = y_2'(L - l_d, t) = 0. \tag{3}$$

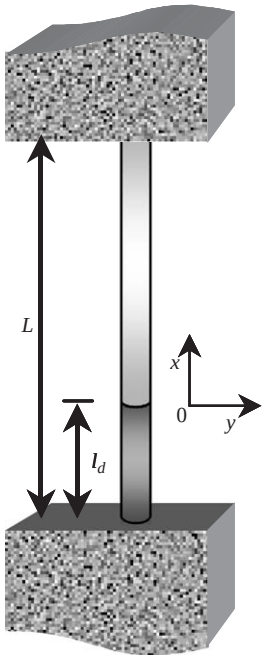

Fig. 1. Schematic representation of a clamped tube partly filled with liquid.

The continuity and equilibrium conditions at the origin are

$$\begin{aligned} y_1(0,t) &= y_2(0,t), \quad y_1'(0,t) = y_2'(0,t), \\ y_1''(0,t) &= y_2''(0,t), \quad y_1'''(0,t) = y_2'''(0,t). \end{aligned} \tag{4}$$

The general solutions of the equation of motion for a uniform beam [8] are

$$y_j(x,t) = \mathbf{C}_j^{\mathrm{T}} \mathbf{G}_j(x) \mathrm{e}^{\mathrm{i}\omega t}, \tag{5}$$

with the displacement function and constants given by

$$\begin{aligned} \mathbf{C}_j^{\mathrm{T}} &= (\, C_{j1} \quad C_{j2} \quad C_{j3} \quad C_{j4} \,), \\ \mathbf{G}_j^{\mathrm{T}}(x) &= (\, \sin k_j x \quad \cos k_j x \quad \sinh k_j x \quad \cosh k_j x \,), \end{aligned} \tag{6}$$

where $k_j^4 = m_j \omega^2 / EI$.

Applying the continuity and equilibrium conditions to the general solution, the following relation is obtained:

$$\mathbf{C}_1 = \mathbf{F}\mathbf{C}_2, \tag{7}$$

with $\mathbf{F}$ given by

$$\mathbf{F} = \begin{pmatrix} \gamma\gamma_1 & 0 & \gamma\gamma_2 & 0 \\ 0 & \gamma_1 & 0 & \gamma_2 \\ \gamma\gamma_2 & 0 & \gamma\gamma_1 & 0 \\ 0 & \gamma_2 & 0 & \gamma_1 \end{pmatrix}, \tag{8}$$

where $\gamma = (m_2/m_1)^{1/4}$, $\gamma_1 = (1+\gamma^2)/2$ and $\gamma_2 = (1-\gamma^2)/2$. Substitution of Eqs. (5) and (7) into the boundary conditions Eq. (3) results in

$$\mathbf{S}\mathbf{C}_1 = 0, \tag{9}$$

with

$$\mathbf{S} = \begin{pmatrix} -\gamma\gamma_1 \sin u_1 - \gamma\gamma_2 \sinh u_1 & \gamma_1 \cos u_1 + \gamma_2 \cosh u_1 & & \\ \gamma\gamma_1 \cos u_1 + \gamma\gamma_2 \cosh u_1 & \gamma_1 \sin u_1 - \gamma_2 \sinh u_1 & & \\ \sin u_2 & \cos u_2 & & \\ \cos u_2 & -\sin u_2 & & \\ & & -\gamma\gamma_2 \sin u_1 - \gamma\gamma_1 \sinh u_1 & \gamma_2 \cos u_1 + \gamma_1 \cosh u_1 \\ & & \gamma\gamma_2 \cos u_1 + \gamma\gamma_1 \cosh u_1 & \gamma_2 \sin u_1 - \gamma_1 \sinh u_1 \\ & & \sinh u_2 & \cosh u_2 \\ & & \cosh u_2 & \sinh u_2 \end{pmatrix}, \tag{10}$$

where $u_1 = k_1 l_d$ and $u_2 = k_2(L-l_d)$. A non-trivial solution is obtained when

$$\det \mathbf{S} = 0. \tag{11}$$

After some rearrangement and simplification, the analytical solution of Eq. (11) is given by

$$\begin{aligned} &(\gamma_1^2 + \gamma_2^2)[1 - \cos u_1 \cos u_2 \cosh u_1 \cosh u_2] + 2\gamma_1\gamma_2[\cos u_1 \cosh u_1 - \cos u_2 \cosh u_2] \\ &\quad + \gamma\gamma_1[\sin u_1 \sin u_2 \cosh u_1 \cosh u_2 - \sinh u_1 \sinh u_2 \cos u_1 \cos u_2] \\ &\quad + \gamma\gamma_2 \cos u_2[\sin u_2 \sinh u_1 \cosh u_2 - \sin u_1 \sinh u_2] \\ &\quad + \gamma^2 \sin u_1 \sin u_2 \sinh u_1 \sinh u_2 = 0. \end{aligned} \tag{12}$$

In the special case of a uniform tube ($l_d = 0$ or $l_d = L$), Eq. (12) reduces to

$$\cos u \cosh u = 1 \tag{13}$$

for $\gamma \neq 0$, with $u = (m_j/EI)^{1/4} L\sqrt{\omega_i}$. Numerically approximated, the solutions of Eq. (13) are $u \approx 0$, 1.5056π, 2.4998π and $u \approx (n+\frac{1}{2})\pi$ for $n = 3, 4, 5\ldots$ where n corresponds to the vibrational mode. The Bernoulli–Euler theory is only applicable to long slender beams. For beams with compact cross sections, shear and rotation cannot be neglected. For smaller wavelengths, the Bernoulli–Euler theory is extended to the Timoshenko beam theory, which includes shear and rotation [9]. The difference in the frequency of the fundamental mode predicted by the Bernoulli–Euler and Timoshenko theories depend strongly on the types of support. For uniformly loaded double clamped beams with a length-diameter ratio of more than 50, the predicted fundamental mode frequency differs less than 5% [10].

3. Experimental

The experimental setup, shown in Fig. 2, consists of a steel capillary ($\rho_{\text{steel}} = 7950\,\text{kg/m}^3$) clamped by two 20 mm clamps. The distance between the clamps is 160 mm. The capillary has inner and outer diameters of 1.0 and 3.2 mm, respectively. At the bottom, the steel capillary is

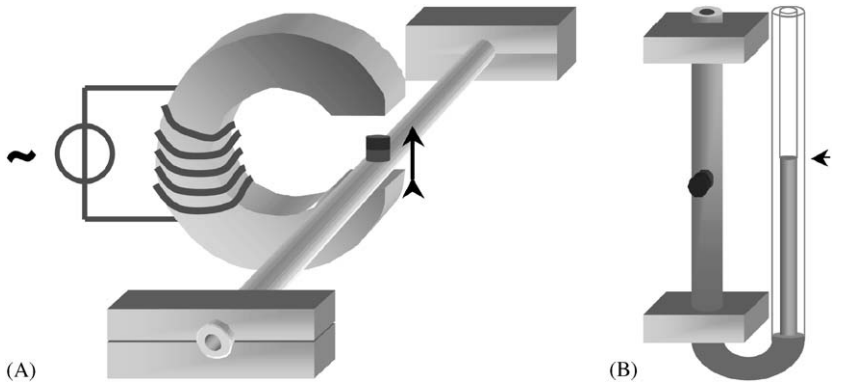

Fig. 2. Schematic view of the experimental setup. (A) Clamped tube configuration with attached magnet, coil and impedance meter. (B) Test setup with clamped steel capillary at the left side and a glass capillary at the right side, connected by flexible tubing.

connected to a glass capillary by flexible tubing. The glass capillary has inner and outer diameters of 2.1 and 3.9 mm, respectively. The two connected tubes are partly filled with mercury ($\rho_{\text{mercury}} = 13540\,\text{kg/m}^3$). To excite the steel tube, a small magnet ($m = 0.15\,\text{g}$) is attached to the center. The magnetic field of the magnet is perpendicular to the axis of the tube and in line with the slit in the toroid coil, as shown in Fig. 2A. The coil is connected to an impedance analyzer (Hioki 3532 LCR, ± 0.1 Hz), controlled by a computer. The resonance frequency of the tube is obtained from a maximum in the spectrum of the coil impedance modulus. This setup allows measurement of the odd modes of vibration, containing an antinode at half the tube length. The resolution of the frequency setting on the analyzer is 0.1 Hz in the low frequency range. In the high frequency range, the resolution is 1 Hz, which is too large to detect the higher modes of vibration. The mercury level in the glass tube is visually observed using a cathetometer (Bleeker, ± 0.1 mm).

4. Results and discussion

4.1. Tube partially filled with mercury

In Fig. 3 the shift in frequency for the fundamental mode of a steel tube partly filled with mercury is shown. The experimental data are correlated with the Bernoulli–Euler model. In the specified setup, with $m_1/m_2 \approx 1.184$ ($\gamma \approx 0.956$), the frequency shifts from 509.9 to 468.5 Hz. Calculating the bending stiffness EI of the tube from the frequency of the empty tube and applying the tube dimensions and material densities, a shift of the frequency to 468.54 Hz is predicted. As shown in Fig. 3, the model excellently relates the filled tube frequency to the empty tube frequency. However, for partially filled tubes, the experimental data appear to be shifted to lower filling heights. This is caused by the capillary action of mercury in these small tubes, since mercury exhibits a non-wetting behavior on both glass and steel surfaces, causing a negative capillary action. Eq. (14) shows the difference in height between the steel and glass (vertical) tubes,

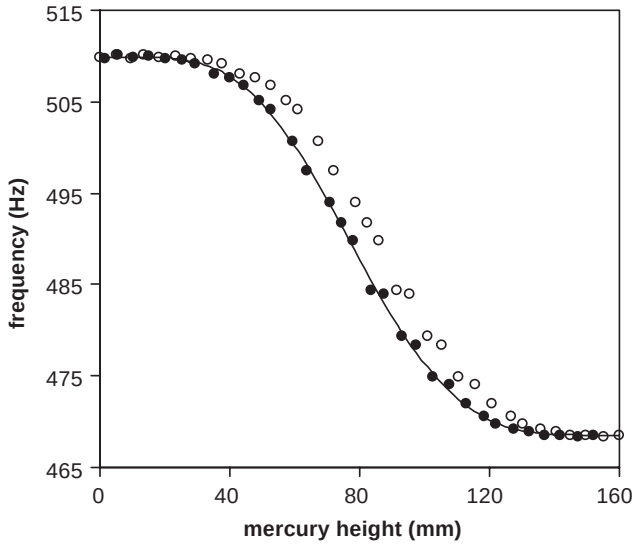

Fig. 3. Resonance frequency as a function of filling height of a steel capillary partly filled with mercury. Data before (○) and after correction for capillary action (●, ca), and the correlation with the Bernoulli–Euler model (—) is shown.

which is caused by capillary action:

$$\mathrm{d}h = \frac{2\gamma}{\rho g}\frac{r_1 \cos\ \theta_{c,2} - r_2 \cos\ \theta_{c,1}}{r_1 r_2}. \tag{14}$$

Here γ is the surface tension, θ is the contact angle and r are the tube radii. After correction of the experimental data for capillary action, excellent agreement between the model calculations and the data is observed. At least for the fundamental mode, these results justify the assumption that the measured resonance frequency can be described by the natural frequency of the tube. Furthermore, in the applied setup the mass of the magnet attached to the tube appears not to have a measurable influence on the characteristics of the response of the resonance frequency to changing fluid heights. For application of the technique as an indicator for liquid levels in a tube, only the fundamental mode is applicable. The plateaus occurring at higher modes result in regions with a very small gradient in frequency. For the same reason, practical measurements of fluid levels are limited to the midsection of the tube, approximately $0.25 < l_d/L < 0.75$, thus limiting the effective measuring region of the tube to half the tube length.

The effects of finite transversal and rotational stiffness of the clamps on the measurement accuracy have not been addressed in this study. However, these effects may be relevant for prolonged measurement times, and are therefore subject to further study.

4.2. Model analysis

The relative frequency change as a function of filling height is calculated by Eq. (11) or (12), respectively. In Fig. 4 the frequency ratios as a function of the relative filling height are shown for

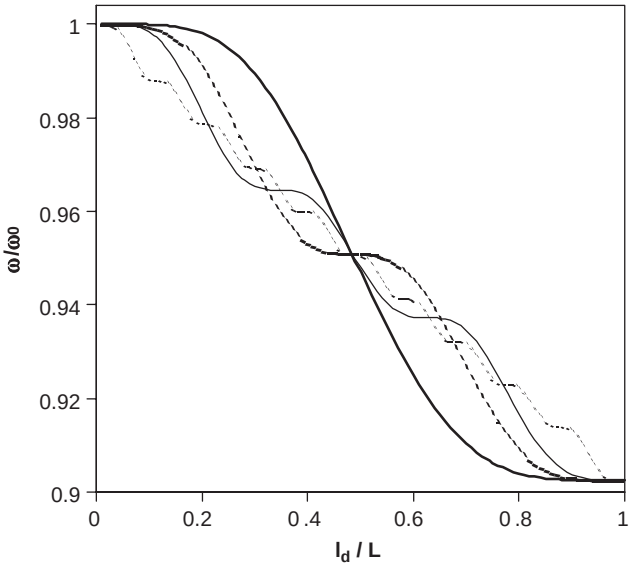

Fig. 4. Bernoulli–Euler model calculations of the relative frequency change as a function of relative filling height of the tube, with $\gamma = 0.95$ ($m_1/m_2 \approx 1.228$). Vibrational modes 1 (——), 2 (■■■), 3 (—) and 10 (- - -) are shown.

vibrational modes 1, 2, 3 and 10. Mode 10 is the highest mode, which can be described with the Bernoulli–Euler theory. In the calculations $\gamma = 0.95$ is used, corresponding to a relative mass density increase of 22.77%. All modes show the same relative change in frequency for a fully filled tube. Similar behavior was observed for simply supported [6] and clamped-free [7] geometries.

For the fundamental mode, a continuous decrease of the frequency with increasing fluid levels is observed, with a steep gradient near a relative filling height of 0.5. At higher vibrational modes, regions of non-varying frequencies (plateaus) are observed. These plateaus can be attributed to the occurrence of vibrational nodes. The fundamental mode contains no nodes. For higher modes, each mode adds an additional node. Near a node, displacements and accelerations are small, resulting in less added mass effects. The reverse is true near antinodes, where accelerations are large and a significant shift in frequency with increasing fluid height is observed.

Though symmetric boundary conditions are applied, the curves for all modes are slightly asymmetric, due to the asymmetric mass distribution of the tube. For all modes, the central node or antinode is slightly shifted towards the fluid filled side. The actual shift in mode shape depends on the mass density ratio and the filling height. In Fig. 5A, the fundamental mode shape is shown for a relative filling height of 0.5 and a γ of 0.7, which corresponds to an increase in mass density of 316.5%. Such a large difference in mass densities combined with the fluid level near the antinode, results in a large shift in the position of the antinode towards the filled side of the tube. In Fig. 5B, the shift in mode shape is shown as a function of filling height of the tube. In these calculations, a more moderate mass density ratio of 1.229 ($\gamma = 0.95$) is applied, resulting in smaller changes in mode shape. The largest shifts of the antinode are observed for filling heights near the antinode (l_d/L)$\sim$0.5, where displacements are large. The shift in frequency for a filled tube is a unique function of the mass density ratio of the two sides of the tube. The ratio is related to tube

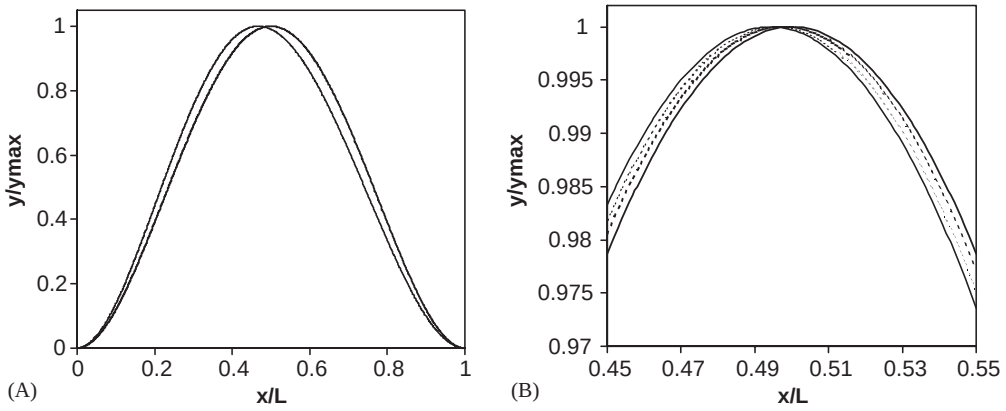

Fig. 5. Shifts in the fundamental mode shape $y(x)$. (A) Mode shape of a half filled tube with $\gamma = 0.7$ (—, $m_1/m_2 = 4.165$) and an empty tube (▬). (B) Mode shape as a function of filling height l_d with $\gamma = 0.95$ ($m_1/m_2 = 1.228$) and filling heights $l_d/L = 0$ (▬), 0.3 (▪▪▪), 0.5 (—), 0.6 (- - -).

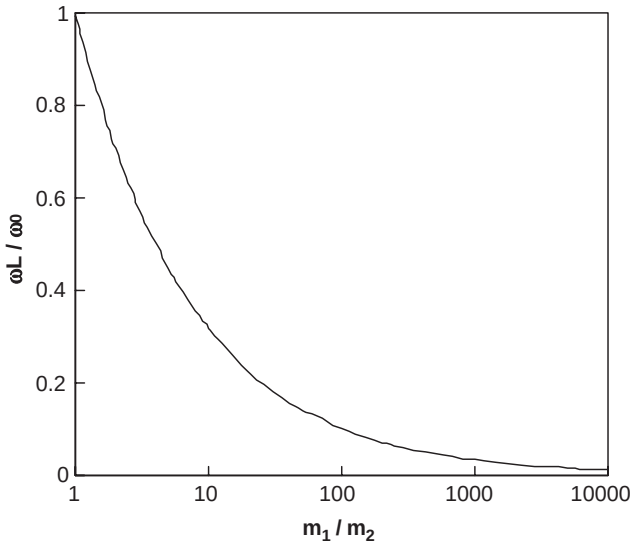

Fig. 6. Relative frequency shift of a filled tube as a function of the relative mass density ratio.

dimensions and material densities by

$$\frac{m_1}{m_2} = \frac{d_{\text{out}}^2 - \left(1 - \frac{\rho_{\text{liquid}}}{\rho_{\text{tube}}}\right) d_{\text{in}}^2}{d_{\text{out}}^2 - d_{\text{in}}^2}. \tag{15}$$

In Fig. 6 the frequency shift of a filled tube is shown as a function of the mass ratios. The frequency shows an asymptotic decline to zero. A reduction in frequency of 50% is already reached for a mass ratio m_1/m_2 of 4. These shifts in relative frequency are the same for all vibrational modes. However, for higher modes the natural frequency of the empty tube increases

quadratically

$$\frac{\omega_n}{\omega_1} = \left(\frac{u_n}{u_1}\right)^2, \tag{16}$$

where n corresponds to the mode number and u_n is the nth solution of Eq. (13), excluding the trivial solution $u = 0$.

4.3. Sensitivity for low density liquids

To obtain insight in the accuracy of measurements with less dense fluids than mercury, the sensitivity of the filling height to a change in frequency has been determined for water in steel high-pressure tubes. For this purpose, the change of the liquid height Δl_d, corresponding to a change in frequency of 0.2 Hz at a filling of $L/l_d = 0.75$ is calculated for three commercially available Swagelock® high-pressure steel tubes with increasing diameters as a function of the length of the tube between the clamps. The tubes have outer diameters (O.D.) of $\frac{1}{8}$, $\frac{1}{4}$ and $\frac{1}{2}$ in and wall thicknesses of 0.028, 0.035 and 0.065 in, respectively, which correspond to the minimum available thickness suitable for a working pressure of 30 MPa at 475 K. In Fig. 7, the results are shown for clamped tube lengths of $10 \times$ O.D. to 160 mm. All tubes show a progressively decreasing accuracy with increasing length of the clamped section. If we accept a maximum Δl_d of 1 mm at an accuracy in the frequency of 0.2 Hz, the maximum lengths are 114 mm for the $\frac{1}{8}$ in tube and 125 mm for the $\frac{1}{4}$ in tube. For the $\frac{1}{2}$ tube, the best achievable accuracy is 1.9 mm at the minimum length of $10 \times$ O.D.. As mentioned above, the maximum detectable range of fluid levels is half these clamped-section lengths. In general, the sensitivity study shows that the operating

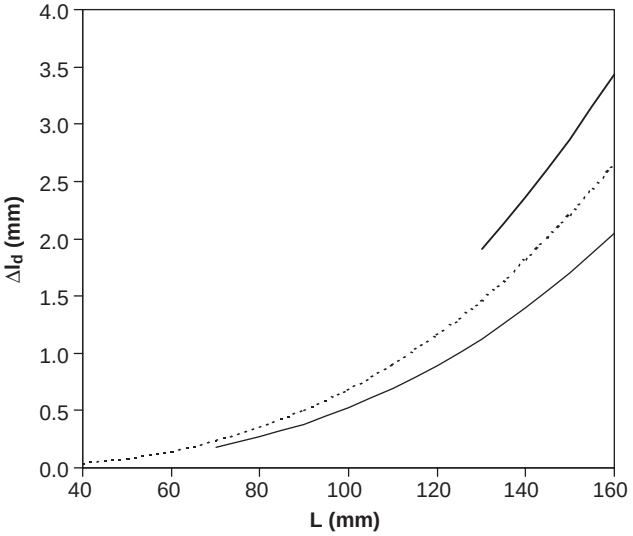

Fig. 7. Sensitivity of the calculated filling height of water at $L/d = 0.75$ to a frequency change of 0.2 Hz as a function of tube length for three commercially available high-pressure steel tubes. (- - - $\frac{1}{8}''$ O.D./0.028″ wall; — $\frac{1}{4}''$ O.D./0.035″ wall; ▬ $\frac{1}{2}''$ O.D./0.065″ wall.)

window of the contactless liquid detection method is sufficiently broad, within the limits of the tube diameter required for the applied pressure.

5. Conclusions

In this work, the use of transversal resonance frequencies as a contactless indication method for the liquid height in a tube has been investigated. A Bernoulli–Euler vibrational analysis for a partly filled tube has been performed, resulting in an analytical solution of the equations of motion. The analysis shows plateau regions in the frequency shift for higher vibrational modes, thus limiting the technique to the fundamental mode. To verify the model calculations, experiments have been carried out on a realistic steel capillary filled with mercury. The model calculations are in good agreement with the data. In the experiments, the use of the complex electrical impedance of a toroid coil enclosing the tube with a magnet attached has proven to be a good indicator for the detection of the natural frequency of the tube. Using the fundamental mode, accurate measurements are limited to the midsection of the tube, where the largest frequency gradient occurs. For detection of mercury in tubes with inner diameters below 10 mm, the capillary action of the mercury has to be taken into account. The experiments indicate a fluid level detection sensitivity adequate for control purposes in industrial automation applications. The constructional simplicity of the method and its contactless setup, as well as the ability to be used in high-pressure systems, makes the technique a versatile tool for fluid level detection in a wide variety of industrial applications such as chemical, pharmaceutical and food processes.

References

[1] M.A. McHugh, V.J. Krukonis, *Supercritical Fluid Extraction: Principles and Practice*, Butterworth Heinemann, Boston, 1993.
[2] A.I. Cooper, Polymer synthesis and processing using supercritical carbon dioxide, *Journal of Materials Chemistry* 10 (2000) 207–234.
[3] B. Subramaniam, R.A. Rajewski, K. Snavely, Pharmaceutical processing with supercritical carbon dioxide, *Journal of Pharmeutical Sciences* 86 (1997) 885–890.
[4] E. Reverchon, Supercritical antisolvent preparation of micro- and nano-particles, *Journal of Supercritical Fluids* 15 (1999) 1–21.
[5] M.A. Jacobs, M.F. Kemmere, Th.W. de Loos, J.T.F. Keurentjes, Polymer-gas interactions, *Proceedings of the Seventh Meeting on Supercritical Fluids*, Antibes, 2000, pp. 243–246.
[6] K.T. Chan, T.P. Leung, W.O. Wong, Free vibration of simply supported beam partially loaded with distributed mass, *Journal of Sound and Vibration* 191 (1996) 590–597.
[7] K.T. Chan, J.Z. Zhang, Free vibration of a cantilever tube partially filled with liquid, *Journal of Sound and Vibration* 182 (1995) 185–190.
[8] R.E.D. Bishop, D.C. Johnson, *The Mechanics of Vibration*, Cambridge University Press, Cambridge, 1960.
[9] K. Marguerre, K. Wölfel, *Mechanics of Vibration*, Sijthoff & Noordhoff, Alphen aan den Rijn, 1979.
[10] S.M. Han, H. Benaroya, T. Wei, Dynamics of transversely vibrating beams using four engineering theories, *Journal of Sound and Vibration* 225 (1999) 935–988.